COUPLED SIMULATION OF FRACTURE MECHANICS AND TRANSPORT OF CHLORID IN CRACKED CONCRETE SUBMITTED TO PERMANENT LOADING

F. TAVARES[1], C. ANDRADE[1], B. CAPRA[2]

[1]CISDEM. (CSIC-UPM) Spain
[2]Oxand- France
Corresponding author: F. Tavares, e-mail: fabianotavares@yahoo.com.br

Key words: Chloride ingress, corrosion-induced cracking, numerical simulation.

Abstract: Several models for chloride ingress are being developed in order to calculate service life of the reinforcement. This work presents a numerical solution to approach the behavior of a highly corroded beam in presence of chloride environment during 26 years. In order to make the study, a comparison of the numerical pattern of fracture with the real specimen found during the experimental test was made and also was compared the real curve charge-displacement with the numerical simulation.

In this work, we apply cohesive and embedded theories of fracture to study the cracking process induced by corrosion. The volume change resulted from oxidation is implemented as a radial displacement imposed at the concrete-steel interface.

The numerical model reproduces also the patterns of the opening of cracks observed in the experimental data of a 26 years old concrete beam exposed to chloride environment supplied by The Commissariat à l'Energie Atomique (CEA) in France where this work was carried out.

1 INTRODUCTION

Chloride-induced corrosion of steel bars in reinforced concrete is considered the major cause of deterioration of structures. When a structure is being corroded, depending on humidity, environmental temperature ([1] [2] [3] [4, 5]), a mixture of iron oxides is formed, generally named "rust" whose composition depends upon de oxygen availability and the chloride concentration in the case of chloride attack, or the pH value in the case of carbonation. The oxides formed vary in relative composition and usually contain ferrous and ferric hydroxides magnetite, and akaganeite or goethite [6]. These oxides are poorly crystallized in the initial stages of corrosion as is shown in figure 1and in several occasion have been identified as "green rust" of colloidal nature.

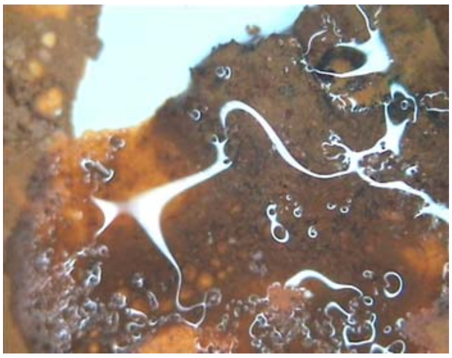

Figure 1: Relative volume of the corrosion products with respect to iron.

The chemical and physical characteristics of the oxides evolve very quickly during the first stages of corrosion due the pore solution chemistry in the corroding spots also evolve and their aspect and composition is not a fixed one but is a mix of several iron oxides. Their consistence is similar to that of a suspension. Regarding their volume, the variation from 1 to around 7 times of the parent iron is related to the theoretical volumes of the oxides once crystalized but during a corrosion process in presence of water and depending on the pH these relations cannot be applied. They precipitated particles are not well crystallized or even they are partially colloidal micelles which move away from the bar by diffusion and migration.

For the case of present work, it is well-know that, this increase in volume, one the one hand, builds up pressure at the steel-concrete interface, together with the frictional effects, the bond strength is enhanced; on the other hand, it exerts tensile stresses in the surrounding concrete and leads to cracking and spalling of the concrete cover [7]. Once the cracked cover releases completely the built-up pressure at the interface, the bond strength deteriorates rapidly. This has been confirmed by experimental data (see for example, [8] [9] [10]), which showed that the ultimate bond strength initially increased with an increase in the degree of corrosion, until it attained a maximum value of about 4% rebar corrosion (or steel weight loss), then it decreased rapidly with an increase in the corrosion level.

On the other hand when a steel rebar is being corroded, the process is not necessarily uniform, actually pitting occurs at the interface, Torres-Acosta et al. [11,12,13,14, 15] have shown that it is the maximum pitting depth, not the average penetration that is the most important parameter affecting the flexural-load capacity reduction in corroded beams.

The objective of this work is to approach by finite elements methodology the behavior of a highly corroded beam in presence of chloride environment during 26 years in order to study the comparison of the numerical pattern of fracture with the real one found during the experimental test and also compare the real curve charge-displacement with the numerical simulation.

In this work, we apply cohesive and embedded theories of fracture to study the cracking process induced by corrosion. The volume change resulted from oxidation is implemented as a radial displacement imposed at the concrete-steel interface.

This work will be presented in five parts.

1 – Introduction

2 – Description of the experimental procedure carried out to verify the mechanical behavior of long-term corroded reinforced concrete beam.

3 – Numerical simulation of the chloride diffusion through the concrete cover found dissolved in the salt fog until reach a critical value at the surface of the layer concrete-rebar. This simulation is important because the experimental report affirmed that the corrosion has been much more intense in the zone of traction and very low in the compression zone. According to the calculations of chloride penetration achieved in this work, the critical chloride concentration reach the rebar just after 24 years. However, as the beam was placed from the beginning of the experimental test in a chamber in presence of salt fog and beside under mechanical load. Such load induced micro cracks that appeared in the concrete in the zone of traction thus increasing the penetration of chlorine through its crack until reaches the critical concentration in a

period of less than one year. And this phenomenon does not appear in compression zone.

4 - To save computational resources, a simulation of the fracture behavior in two-dimensional has been carried out in a section of the beam to determine the pattern of fracture caused by the increase in volume of the corrosion products that has been confirmed by the experimental tests. To accomplish this simulation was used cohesive elements of fracture in order to check how growths the cracks until to be visible on the surface of the concrete cover.

5 - To simulate the behavior of the beam on both action of the external load and the internal load caused by the corrosion products a 3-D simulation has been performed using elements of imbedded fracture in order to plot the curve of the deflection of the central region of the beam versus the external load to compare with the experimental data.

2 EXPERIMENTAL PROCEDURE

The experimental program was started at Laboratoire Matériaux et Durabilité des Constrtuction in INSA-Toulouse using reinforced concrete specimens presented in figure 2 .

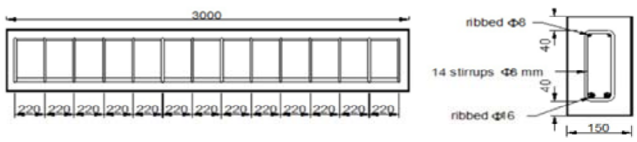

Figure 2: The layout of reinforced concrete beam.

The compositions of concrete and is used to performed this test is specified below:

- 1220 kg/m3 of Rolled gravel (silica + limestone) with size of 5/15 mm.
- 820 kg/m3 of Sand with size of 0/5 mm
- 400 kg/m3 of Portland Cement: OPC HP (high perform)
- 200 kg/m3 of Water

The mechanical property obtained on cylinder specimens (110×220 mm) were:

- The average compressive strength : 45 MPa at 28 days.
- The average elastic modulus : 32 GPa at 28 days.

Unfortunately the energy of fracture of the concrete was not declared on the paper presented by INSA. In this case a value of 150 N/m will be taken in order to carry out the numerical simulation.

2.1 Cycle of environment condition:

The beams were kept in aggressive chloride environment. The aggressive environment was a salt fog (35g/l of NaCl corresponding to the salt concentration of sea water) generated through the use of four sprays located in each upper corner of a confined room (Figure 3). After 6 years of storage, the beams were subjected to wetting–drying cycles in order to accelerate the corrosion process:

- 0 to 6 years: continuous spraying under laboratory conditions (T°≈20°C),
- 6 to 9 years: cycles spraying under laboratory conditions (T°≈20°C), one week of spraying and one week of drying.
- 9 to 19 years: cycles spraying, one week of spraying and one week of drying, however the confined room was transferred outside, so the beams were exposed to the temperature of the south-west of France climate, ranging from -5°C to 35°C.
- 19 to 26 years: cycles have been stopped, unloaded, the beams submitted to the temperature of the southwest of France and had corroded naturally.

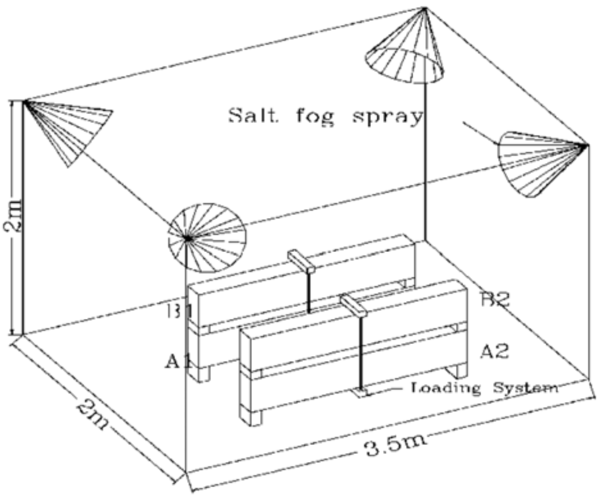

Figure 3: Environment an load condition of the bean.

The beams were loaded in a three-point flexure by coupling a type A beam with a type B beam (beam type B was not considered in this work) (see Figure 2). According to French standards the loading level (M=21.2kN m) for type A beams corresponds to the working load determined at ultimate load limit state ULS.

During the first period of 6 years, the loading level was checked by a device using strain gauges and springs to allow a constant load in spite of creep of concrete. After 6 years, creep effects were smaller and then the load was not re-adjusted with time.

3 NUMERICAL SIMULATION OF THE CHLORIDE DIFFUSION

The numerical simulation of the chloride diffusion were carried out because of the fact that in the experimental results there are no important crack on the surface located in the compressive zone. Such phenomenon occur because of the fact that the beam was placed since of the beginning the beginning of the experimental test in a chamber in presence of salt fog and also under mechanical load. Such load induced micro cracks that appeared in the concrete in the zone of traction thus increasing the penetration of chlorine through its crack until reaches the critical concentration faster than the concentration found on the compression zone.

The initial mesh is generated by GMSH using quadratic six-node finite element. During the simulation this initial mesh is going to be changed into two different meshes to couple the chloride diffusion process and the mechanical behaviour of the concrete crack caused by the corrosion process. The diffusional mesh is formed dividing each quadratic six node element into 4 three node linear element. The mechanical mesh is formed duplicating each node to insert a cohesive quadratic element between 2 quadratic six node element of the initial mesh as shown in figure 4.

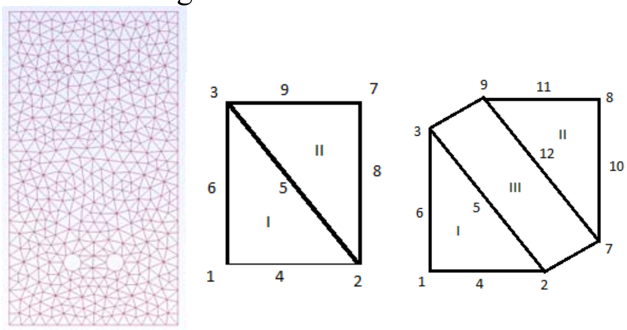

(a) (b) (c)

Figure 4: Initial Mesh used in two dimensions.

The numerical solution has been done using the solver OOFEM controlled entirely by a interface developed during this work by the IETCC. This interface controls during the simulation how the property of the diffusion/mechanical behaviour change during the time and this interface and also re-mesh the geometry to make possible to insert the cohesive element changing the initial mesh. The surface concentration of chloride and the humidity changes during the cycles between the 6 and 9 years of test is take into account.

We assumed a value for the apparent chloride diffusion coefficient of 1.0E-12m2/s for a element not cracked and 1.0E-10 if the element is totally cracked using a linear relation. We also assumed a value of 0.875% wc taking into account the concentration of chloride of the salt fog (34g/l) and the concrete porosity of 10% using the equation below:

Cs = 34g/l*Vol*porosity/(Mass of cement)

In resume, in two dimensions the entire service life of the beam was taken into account.

To perform this simulation we need to assume a value for the critical concentration of chloride to begin the propagation period. For this simulation the threshold values assumed is 0,4 % wc.

The figure 5 shows that such threshold values would be reach in about 24 years if no micro-cracks is considered on the tensile zone. Those explain the reason that the reinforcement located on compressive zone had a low amount of corrosion after 26 years.

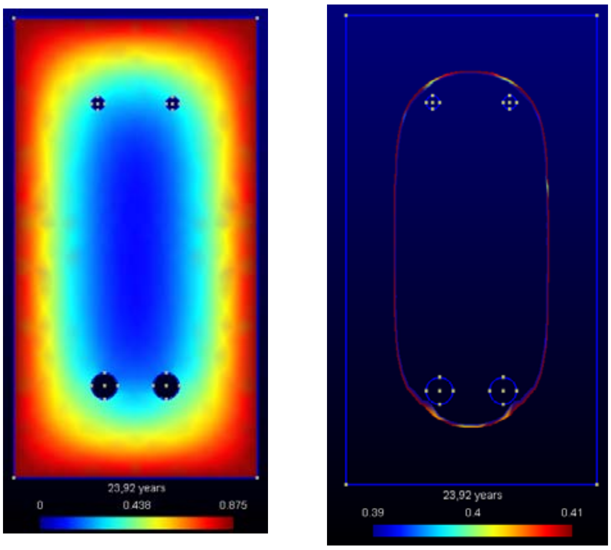

(b) (B)

Figure 5: Chloride concentration distribution not considering the presence of the micro-craks after 24 years.

Taking into account presence of micro-cracks located in tensile zone since of the beginning of the simulation. We can see in figure 6 (a) that the chloride concentration around the rebars at tensile zone is much higher (about 100 times) than those found on profile (A). It happens because the micro-cracks increase up to 100 times the chloride diffusion coefficient.

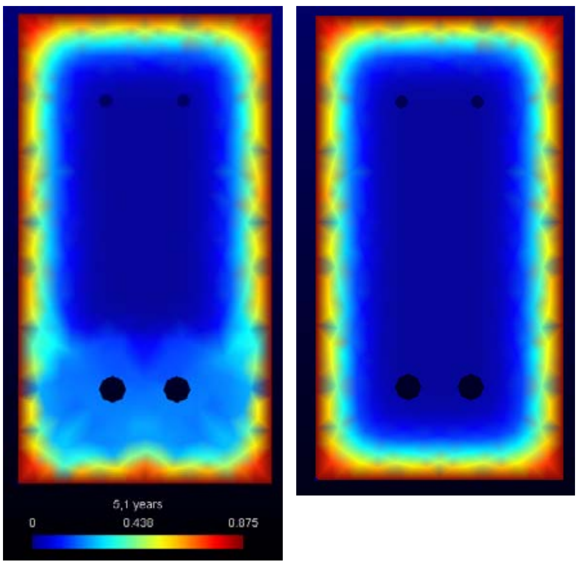

(a) (A)

Figure 6: (a) Chloride concentration distribution considering the presence of micro-cracks found since of the beginning caused by the external loads. (A) Chloride concentration distribution not considering the presence of the micro-craks.

3.1 The pattern of fracture

To save computational resources, a simulation of the fracture behavior in two-dimensional has been carried out in a section of the beam to determine the pattern of fracture caused by the increase in volume of the corrosion products that has been confirmed by the experimental tests. To accomplish this simulation was used cohesive elements of fracture in order to check how growths the cracks until to be visible on the surface of the concrete cover.

Loss of diameter of reinforcement

To perform the numerical simulation is very important to know the loss of diameter of reinforcement to put as a input data for the simulation. The experimental test provided by INSA shows (figure 7) that the average loss of diameter on both front and back side bars at failure location is 21.6%. It means that if we consider that for reinforcements located at the tensile zone begin to corrode since of the beginning of the test. The rate of loss of diameter is 132 micras per year.

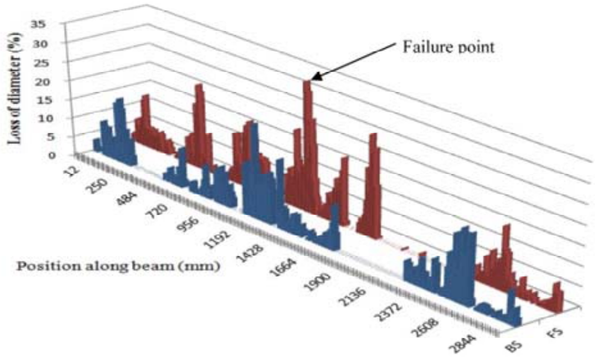

Figure 7: Loss of diameter of reinforcement along the length.

With this simulation we represent the crack pattern of a slice of the beam as we can see in the figure 8 that the numerical specimen represent the real crack pattern found on the real beam.

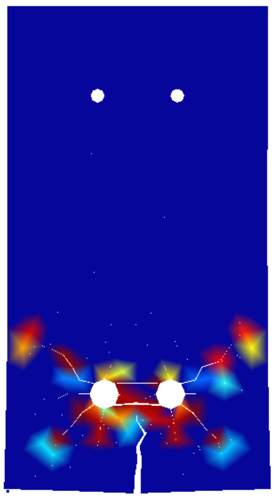

(a)

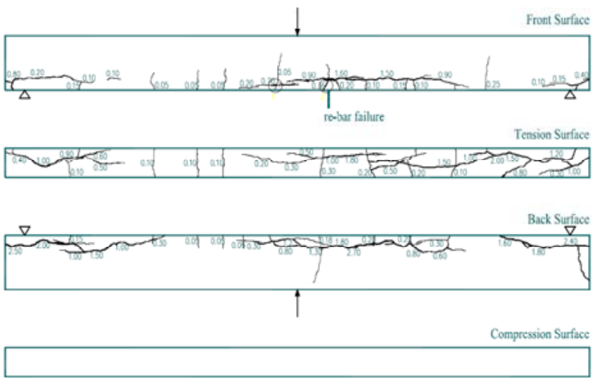

(b)

Figure 8: Crack pattern of the beam

3.2 3D Simulation

To simulate the behavior of the beam on both action of the external load and the internal load caused by the corrosion products a 3-D simulation has been performed using elements of imbedded fracture in order to plot the curve of the deflection of the central region of the beam versus the external load to compare with the experimental data.

The numerical simulation in three dimensions was carried out to take into account the load history applied to the beam. But in this case, just the propagation period has been taken into account. We assumed that all the rebar has uniform corrosion and a uniform corrosion current. The mesh was generated using Linear 3d eight – node finite elements divided into three different zones:

- Concrete bulk : Rotating crack model for concrete Virgin material is modeled as isotropic linear elastic material (described by Young modulus and Poisson ratio). The onset of cracking begins, when principal stress reaches tensile strength. Further behavior is then determined by linear softening law, governed by principle of preserving of fracture energy Gf . For large elements, the tension strength can be articially reduced to preserve fracture energy. The transition to scalar damage model takes place, when the softening stress reaches the specified limit. Multiple cracks are allowed. The elastic unloading and reloading is assumed. In compression regime, this model correspond to isotropic linear elastic material.
- Rebar: Rotating crack model for Steel.
- Interface concrete/rebar : this zone uses the same material of the concrete bulk, but works like a 1mm thick ring to simulate the lost of adherence when this zone is cracked.

To perform the relation between the deflection of the beam an its load , a 3d numerical simulation has been performed.

The problem of this kind of simulation is the fact that is very expensive in time for the computer.

On figure 9 we can see the curve of the relation between the deflection of the central region of the beam and the external load. It can be remarked that the numerical simulation present a rigidity of the beam lower than the real experement. Such phenomena happens because of some possible causes: The energy o fracture was not measured. We have seen that the loss of diameter is not homogeneous along the rebars. And for this simulation we have taken the average value on the crack zone.

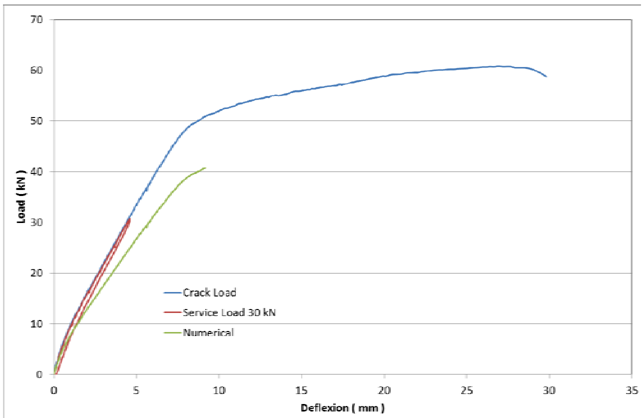

Figure 9: Curve of the deflection of the central region of the beam versus the external load (numerical and experimental data)

4 CONCLUSION

The 2D simulation of Chloride diffusion in presence of micro-cracks on the tensile zone enabled to identify the possible cause of the difference between the corrosion-induced crack on the tensile and compression zone.

Corrosion-induced cracking has been studied to model the concrete fracture by means of a cohesive model to take into account the topological change as multiple cracks form and propagate. Present cohesive model has enabled to follow on 2D cracking pattern and how the material is being disintegrated around the bar. This model type then will serve to study the evolution of the crack pattern at further and advanced stages of the corrosion.

The 3D simulation enabled to verify the behaviour of the coupled situation when a external load is applied together with the presence of corrosion process of the rebars to approach the curve of the deflection of the central region of the beam versus the external load and compare with the experimental data.

ACKNOWLEDGEMENTS

The authors are grateful to the facilities provided by the Commissariat à l'Energie Atomique (CEA) in France for developing present work. In particular they are grateful to Allain Millard and Valerie L'Hostis for the support given to F. Tavares during its stay in Saclay installations and for providing the corrosion data of the beams. The authors also acknowledge the funding obtained from the Ministry of Science and Innovation and the CSIC of Spain through the CONSOLIDER-SEDUREC project which had supported the visit of F. Tavares to Oxand – Paris- France.

REFERENCES

[1] Andrade C, Alonso C, Molina FJ. Cover cracking as a function of rebar corrosion.1. Experimental test. Mater Struct. 1993;26(162):453-464.

[2] Andrade C, Alonso C, Sarria J. Influence of relative humidity and temperature on-site corrosion rates. Mater Constr. 1998;48(251):5-17.

[3] Andrade C, Alonso C, Sarria J. Corrosion rate evolution in concrete structures exposed to the atmosphere. Cem Concr Compos. 2002;24(1):55-64.

[4] Andrade C, Castillo A. Evolution of reinforcement corrosion due to climatic variations. Mater Corros. 2003;54(6):379-386.

[5] Andrade C, Martinez I, Zuloaga P. Environmental influence in the corrosion parameters registered in a buried pilot nuclear waste container. J Phys IV. 2006;136:321-329.

[6] Beverskog B, Puigdomenech I. Revised Pourbaix diagrams for iron at 25-300ºC. Corrosion Science vol. 38, no.12, pp 2121-2135.

[7]Coronelli D. Corrosion cracking and bond strength modeling for corroded bars in reinforced concrete. ACI Struct J. 2002;99(3):267-276.

[8] Almusallam AA, AlGahtani AS, Aziz AR, Rasheeduzzafar. Effect of reinforcement corrosion on bond strength. Constr Build Mater. 1996;10(2):123-129.

[9] Amleh L, Ghosh A. Modeling the effect of corrosion on bond strength at the steel-concrete interface with finite-element analysis. Canadian Journal of Civil Engineering. 2006;33(6):673-682.

[10] Amleh L, Mirza S. Corrosion influence on bond between steel and concrete. ACI Struct J. 1999;96(3):415-423.

[11] Rodriguez J, Ortega LM, Casal J. Load carrying capacity of concrete structures with corroded reinforcement. Constr Build Mater. 1997;11(4):239-248.

[12] Ruiz G, Elices M, Planas J. Size effect and bond-slip dependence of lightly reinforced concrete beams. Minimum Reinforcement in Concrete Members. 1999;24:67-97.

[13] Ruiz G. Propagation of a cohesive crack crossing a reinforcement layer. Int J Fract. 2001;111(3):265-282.

[14] Torres-Acosta AA, Martinez-Madrid M. Residual life of corroding reinforced concrete structures in marine environment. Journal of Materials in Civil Engineering. 2003;15(4):344-353.

[15] Torres-Acosta AA, Navarro-Gutierrez S, Teran-Guillen J. Residual flexure capacity of corroded reinforced concrete beams. Engineering Structures. 2007;29(6):1145-1152.

[16] Cabrera JG. Deterioration of concrete due to reinforcement steel corrosion. Cem Concr Compos. 1996;18(1):47-59.

[17] Castel A, Francois R, Arliguie G. Mechanical behaviour of corroded reinforced concrete beams - Part 1: Experimental study of corroded beams. Mater Struct. 2000;33(233):539-544.

[18] Coronelli D, Gambarova P. Structural assessment of corroded reinforced concrete beams: Modeling guidelines. J Struct Eng-ASCE. 2004;130(8):1214-1224.

[19]Bhargava K, Ghosh AK, Mori Y, Ramanujam S. Corrosion-induced bond strength degradation in reinforced concrete - Analytical and empirical models. Nucl Eng Des. 2007;237(11):1140-1157.

[20] Dagher HJ, Kulendran S. Finite-element modeling of corrosion damage in concrete structures. ACI Struct J. 1992;89(6):699-708.

[21] El Maaddawy T, Soudki K, Topper T. Computer-based mathematical model for performance prediction of corroded beams repaired with fiber reinforced polymers. Journal of Composites for Construction. 2005;9(3):227-235.

[22] Berra M, Castellani A, Coronelli D, Zanni S, Zhang G. Steel-concrete bond deterioration due to corrosion: finite-element analysis for different confinement levels. Mag Concr Res. 2003;55(3):237-247.

[23] Lundgren K. Modelling the effect of corrosion on bond in reinforced concrete. Mag Concr Res. 2002;54(3):165-173.

[24] Bhargava K, Ghosh AK, Mori Y, Ramanujam S. Analytical model for time to cover cracking in RC structures due to rebar corrosion. Nucl Eng Des. 2006;236(11):1123-1139.

[25] Xu G, Wei J, Zhang KQ, Zhou XW. A calculation model for corrosion cracking in RC structures. Journal of China University of Geosciences. 2007;18(1):85-89.

[26] Bhargava K, Ghosh AK, Mori Y, Ramanujam S. Model for cover cracking due to rebar corrosion in RC structures. Engineering Structures. 2006;28(8):1093-1109.

[27] Vidal T, Castel A, Francois R. Analyzing crack width to predict corrosion in reinforced concrete. Cem Concr Res. 2004;34(1):165-174.

[28] Du YG, Chan AHC, Clark LA. Finite element analysis of the effects of radial expansion of corroded reinforcement. Computers & Structures. 2006;84(13-14):917-929.

[29] El Maaddawy T, Soudki K. A model for prediction of time from corrosion initiation to corrosion cracking. Cem Concr Compos. 2007;29(3):168-175.

[30] Ruiz G, Ortiz M, Pandolfi A. Three-dimensional finite-element simulation of the dynamic Brazilian tests on concrete cylinders. Int J Numer Methods Eng. 2000;48(7):963-994.
[31] Ruiz G, Pandolfi A, Ortiz M. Three-dimensional cohesive modeling of dynamic mixed-mode fracture. Int J Numer Methods Eng. 2001;52(1-2):97-120.
[32] Ortiz M, Pandolfi A. Finite-deformation irreversible cohesive elements for three-dimensional crack-propagation analysis. Int J Numer Methods Eng. 1999;44(9):1267-1282.
[33] Yu RC, Ruiz G. Explicit finite element modeling of static crack propagation in reinforced concrete. Int J Fract. 2006;141(3-4):357-372.
[34] Ahmed SFU, Maalej M, Mihashi H. Cover cracking of reinforced concrete beams due to corrosion of steel. ACI Mater J. 2007;104(2):153-161.
[35] Wang XH, Liu XL. Modeling bond strength of corroded reinforcement without stirrups. Cem Concr Res. 2004;34(8):1331-1339.
[36] Pantazopoulou SJ, Papoulia KD. Modeling cover-cracking due to reinforcement corrosion in RC structures. Journal of Engineering Mechanics-Asce. 2001;127(4):342-351.
[37] Camacho GT, Ortiz M. Computational modelling of impact damage in brittle materials. International Journal of Solids and Structures. 1996;33(20-22):2899-2938.
[38] Molina FJ, Alonso C, Andrade C. Cover cracking as a function of rebar corrosion. 2. Numerical model. Mater Struct. 1993;26(163):532-548.
[39] Inamullah Khan, Raoul François and Arnaud Castel. Mechanical Behavior of Long-Term Corroded Reinforced Concrete Beam. RILEM Bookseries 5, 2011:243-258.